AMERICAN SOCIETY FOR MICROBIOLOGY | mBio®

RESEARCH ARTICLE

SARS-CoV-2 Exposure in Norway Rats (*Rattus norvegicus*) from New York City

Yang Wang,[a,b,c] Julianna Lenoch,[d] Dennis Kohler,[d] Thomas J. DeLiberto,[e] Cynthia Y. Tang,[a,b,c] Tao Li,[f] Yizhi Jane Tao,[g] Minhui Guan,[a,b,c] Susan Compton,[h] Caroline Zeiss,[h] Jun Hang,[f] Xiu-Feng Wan[a,b,c,i]

[a]Center for Influenza and Emerging Infectious Diseases, University of Missouri, Columbia, Missouri, USA
[b]Department of Molecular Microbiology and Immunology, School of Medicine, University of Missouri, Columbia, Missouri, USA
[c]Bond Life Sciences Center, University of Missouri, Columbia, Missouri, USA
[d]USDA APHIS Wildlife Services National Wildlife Disease Program, Fort Collins, Colorado, USA
[e]USDA APHIS Wildlife Services, Fort Collins, Colorado, USA
[f]Viral Diseases Branch, Walter Reed Army Institute of Research, Silver Spring, Maryland, USA
[g]Department of BioSciences, Rice University, Houston, Texas, USA
[h]School of Medicine, Yale University, New Haven, Connecticut, USA
[i]Department of Electrical Engineering & Computer Science, College of Engineering, University of Missouri, Columbia, Missouri, USA

ABSTRACT Millions of Norway rats (*Rattus norvegicus*) inhabit New York City (NYC), presenting the potential for transmission of severe acute respiratory syndrome coronavirus 2 (SARS-CoV-2) from humans to rats. We evaluated SARS-CoV-2 exposure among 79 rats captured from NYC during the fall of 2021. Our results showed that 13 of the 79 rats (16.5%) tested IgG- or IgM-positive, and partial SARS-CoV-2 genomes were recovered from all 4 rats that were qRT-PCR (reverse transcription-quantitative PCR)-positive. Genomic analyses suggest these viruses were associated with genetic lineage B, which was predominant in NYC in the spring of 2020 during the early pandemic period. To further investigate rat susceptibility to SARS-CoV-2 variants, we conducted a virus challenge study and showed that Alpha, Delta, and Omicron variants can cause infections in wild-type Sprague Dawley (SD) rats, including high replication levels in the upper and lower respiratory tracts and induction of both innate and adaptive immune responses. Additionally, the Delta variant resulted in the highest infectivity. In summary, our results indicate that rats are susceptible to infection with Alpha, Delta, and Omicron variants, and wild Norway rats in the NYC municipal sewer systems have been exposed to SARS-CoV-2. Our findings highlight the need for further monitoring of SARS-CoV-2 in urban rat populations and for evaluating the potential risk of secondary zoonotic transmission from these rat populations back to humans.

IMPORTANCE The host tropism expansion of SARS-CoV-2 raises concern for the potential risk of reverse-zoonotic transmission of emerging variants into rodent species, including wild rat species. In this study, we present both genetic and serological evidence for SARS-CoV-2 exposure to the New York City wild rat population, and these viruses may be linked to the viruses that were circulating during the early stages of the pandemic. We also demonstrated that rats are susceptible to additional variants (i.e., Alpha, Delta, and Omicron) that have been predominant in humans and that susceptibility to infection varies by variant. Our findings highlight the reverse zoonosis of SARS-CoV-2 to urban rats and the need for further monitoring of SARS-CoV-2 in rat populations for potential secondary zoonotic transmission to humans.

KEYWORDS SARS-CoV-2, rat coronavirus, Norway rats, *Rattus norvegicus*, brown rats, rat COVID-19, surveillance, reverse zoonosis, Delta, Omicron, wildlife

Editor John A. Lednicky, University of Florida

Address correspondence to Xiu-Feng Wan, wanx@missouri.edu, or Thomas J. DeLiberto, thomas.j.deLiberto@usda.gov.

The authors declare no conflict of interest.

Received 30 December 2022
Accepted 7 February 2023
Published 9 March 2023

As of 10 October 2022, severe acute respiratory syndrome coronavirus 2 (SARS-CoV-2), the virus responsible for coronavirus disease 2019 (COVID-19), has caused approximately 621 million human cases and 6.6 million deaths globally (1). In addition to humans, a wide range of wild, domestic, and captive animals have been documented with exposure to SARS-CoV-2, including deer, mink, otters, ferrets, hamsters, gorillas, cats, dogs, lions, and tigers (2–4). SARS-CoV-2 detected in farmed mink was shown to have directly caused infections in humans (5), highlighting mink as a potential reservoir for secondary zoonotic infections.

SARS-CoV-2 has undergone rapid evolution, and many genetic variants have been identified, including several variants of concern (VOC), such as Alpha (B.1.1.7 lineage), Beta (B.1.351 lineage), Gamma (P.1 lineage), Delta (B.1.617.2 and AY sublineages), and Omicron (B.1.1.529 and BA sublineages). The Alpha, Beta, and Gamma variants acquired substitutions at the receptor-binding domain (RBD) of the spike protein that were reported to facilitate infectivity in mice and/or rats compared to the original pandemic strain (6–9). The tropism expansion of SARS-CoV-2 raises a concern for the potential risk of reverse-zoonotic transmissions of emerging variants to rodent species, including wild mouse and rat species (10). Two independent SARS-CoV-2 surveillance studies among wild rats from sewage systems in Belgium (late fall of 2020) and Hong Kong (spring of 2021) suggested possible exposure of these animals to SARS-CoV-2, but no viral RNA was detected in the Norway rats that were collected from these studies (11, 12). With the continuing emergence of new SARS-CoV-2 variants, it is still unknown whether the more recent variants of concern (e.g., Delta and Omicron) can infect rats.

In this study, we investigated the exposure of wild rats to SARS-CoV-2 in New York City (NYC), New York, United States. We focused on Norway rats (*Rattus norvegicus*), which make up the predominant wild rat populations in NYC. In addition, we evaluated the capability of Alpha, Delta, and Omicron variants to infect rats.

RESULTS

Detection of SARS-CoV-2 virus in NYC rats. To evaluate whether wild rats have been exposed to SARS-CoV-2, we conducted SARS-CoV-2 surveillance in Norway rats in NYC from 13 September to 16 November 2021, when the Delta variant was predominant in humans in NYC (https://coronavirus.health.ny.gov/covid-19-variant-data). A total of 79 rats inhabiting three sampling sites in Brooklyn, NYC were captured and sampled. Using an in-house enzyme-linked immunosorbent assay (ELISA), we identified 9 out of 79 (11.4%) IgG-positive rat serum samples and 4 IgM-positive samples (5.1%) against both spike and RBD of hCoV-19/Wuhan-Hu-1/2019 (Wuhan-Hu-1) (Table 1). All 13 seropositive samples were subjected to microneutralization assays against the B.1 lineage and the Alpha and Delta variants. However, all samples were negative for neutralizing antibodies. As a negative control, we used ELISA to examine 9 negative serum samples from uninfected Sprague Dawley (SD) rats and 6 serum samples from SD rats infected with one of two rat coronaviruses, sialodacryoadenitis virus (SDAV) or Parker's rat coronavirus (RCV) (13); none exhibited IgG- or IgM-positivity against either spike protein or RBD (data not shown).

Of all the respiratory tissues analyzed from the 79 rats, only 4 samples were positive by qRT-PCR (reverse transcription-quantitative PCR) against both N1 and N2 primers using the CDC SARS-CoV-2 diagnostic panel (Table 1). We ruled out the possibility of qRT-PCR cross-reactivity with six strains of murine betacoronaviruses (i.e., SDAV, Parker's RCV, and four other RCV strains: BCMM, WT, NJ, and 3-15-W [14]). It is noteworthy that 2 of these 4 rats (Rats 2 and 19) were both seropositive and viral RNA-positive. In addition, we had 7 inconclusive samples which were positive on either the N1 or N2 primer but not both. We attempted virus recovery for the 4 positive and 7 inconclusive samples by qRT-PCR, and viruses failed to be recovered from all 11 samples through three passages on Vero E6, 293FT/hACE2 + TMPRSS, rat lung epithelial (L2), and rat lung tracheal epithelial cell lines.

After subjecting these 4 qRT-PCR-positive SARS-CoV-2 samples to whole-genome sequencing, partial SARS-CoV-2 genomes were identified in all samples with a viral

TABLE 1 Serology and qRT-PCR data for rats collected in Brooklyn, NYC in 2021[a]

			ELISA A_{450}/cutoff[b]					
			IgG		IgM		qRT-PCR[c]	
Category	Rat no.	Collection date	Against spike	Against RBD	Against spike	Against RBD	N1	N2
Seropositive	4	Sep 13	1.046	1.001	0.459	0.772	ND	38.42
	40	Sep 16	1.216	1.132	0.591	0.790	ND	ND
	42	Sep 16	1.222	1.049	0.583	0.683	ND	ND
	56	Nov 14	1.397	1.538	0.739	0.629	ND	ND
	59	Nov 14	1.036	1.071	0.550	0.355	ND	ND
	64	Nov 15	1.016	1.199	0.614	0.587	ND	ND
	65	Nov 15	1.163	1.021	1.889	0.591	ND	ND
	20	Sep 13	1.199	0.906	1.554	1.314	ND	ND
	24	Sep 14	0.925	0.721	1.857	1.172	ND	ND
	48	Nov 14	0.308	0.293	1.419	1.373	ND	ND
	79	Nov 16	0.787	0.731	1.174	1.047	ND	ND
qRT-PCR-positive	2	Sep 13	0.238	0.207	0.552	1.063	33.95	34.61
	43	Sep 16	0.573	0.481	0.296	0.323	32.27	34.28
Seropositive and qRT-PCR-positive	19	Sep 13	1.001	1.000	0.480	0.569	36.36	35.83
	46	Sep 16	1.104	1.144	0.587	0.850	35.23	37.31

[a]qRT-PCR, reverse transcription-quantitative PCR; NYC, New York City; ELISA, enzyme-linked immunosorbent assay; RBD, receptor binding domain; A_{450}, absorbance at 450 nm; *CT*, threshold cycle; ND, not detectable.

[b]A_{450}/cutoff was interpreted as negative if $\leq$ 1.0 and seropositive if $>$1.0. The cutoff value was 3-fold of the mean of negative serum samples. Mean value from triplicate measures is shown.

[c]*CT* value was interpreted as positive if $<$40. Mean value from triplicate measures is shown.

genome coverage of 1.6% to 21.3% (Table S1 in the supplemental material). Both molecular characterization and phylogenetic analyses of these partial genomes suggested that the viruses in these rats were associated with genetic lineage B, which was predominant in NYC in the spring of 2020 (Fig. 1).

In addition, we subjected these 4 qRT-PCR-positive and 2 additional inconclusive samples to pan-viral target hybridization enrichment sequencing to identify the presence of any viral genomes in the samples. SARS-CoV-2 sequences were found in 3 out of 4 sequenced qRT-PCR-positive samples (Rats 2, 19, and 43) and one of two inconclusive samples (Rat 38). No sequence data were obtained for the qRT-PCR-positive sample from Rat 46. Interestingly, rat coronavirus was detected in another inconclusive sample (Rat 30) (Table S2). The identified SARS-CoV-2 or rat coronavirus reads aligned with a number of genes across the respective genomes.

Rats displayed varying susceptibility to SARS-CoV-2 variants. The Alpha variant emerged in late 2020 and quickly became a dominant SARS-CoV-2 variant in NYC; subsequently, the Delta and Omicron variants predominated in NYC starting in June and December 2021, respectively (Fig. 2A). To investigate whether these SARS-CoV-2 variants can infect rats, we intranasally challenged 6-week-old wild-type SD rats with Alpha, Delta, or Omicron variants and collected turbinate and lung tissues at 2- or 4-days postinfection (dpi) (Fig. 2B). Compared to the Wuhan-Hu-1 strain, the Omicron variant used in the challenge study possesses the same N501Y substitution on the spike protein as the Alpha variant and 16 additional substitutions, whereas the Delta variant does not possess N501Y, but contains the L452R and T478K substitutions (Fig. 2C).

By 2 and 4 dpi, high levels of viral RNA were detected in both turbinate and lung tissues, and infectious viral titers were detected in turbinate and/or lung tissues, although no body weight loss or other clinical signs were observed in the rats with any of the variants (Fig. 2D to F). In particular, the lungs from the rats infected with the Delta variant showed both the highest RNA copy numbers and the highest infectious viral titers at 2 dpi (RNA copies: $P = 0.0081$ and 0.0060 for Delta versus Alpha and Delta versus Omicron, respectively; infectious viral titers: $P = 0.0287$ and 0.0283 for Delta versus Alpha and Delta versus Omicron, respectively). In addition, antigen expression was detected in

A

Sequence	Pango Lineage (NextClade)	Coverage (%)
hCoV-19/Wuhan/IME-WH05/2019	B	99.7
Rat 2	B	21.3
Rat 19	B	18.4
Rat 43	B	1.9
Rat 46	B	1.6
hCoV-19/USA/NY-Wadsworth-21052117-01/2021	B.1.351 (Beta)	99.1
hCoV-19/USA/NY-NYULH1825/2021	P.1 (Gamma)	98.7
hCoV-19/USA/NY-Wadsworth-21070773-01/2021	B.1.1.7 (Alpha)	99.5
hCoV-19/USA/NY-PRL-2021_1008_02C08/2021	AY.103 (Delta)	98.8
hCoV-19/USA/NY-PRL-2022_0210_00B05/2022	BA.2 (Omicron)	99.6

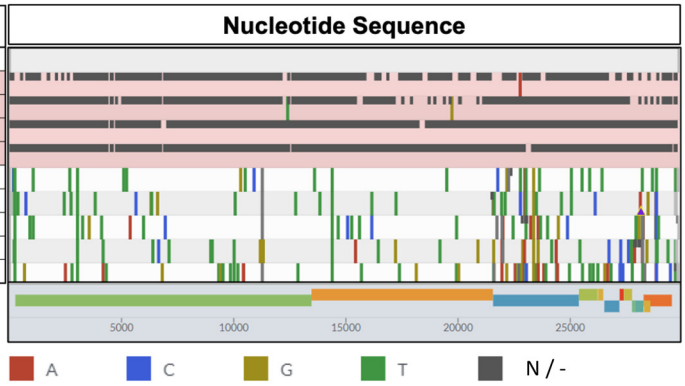

B

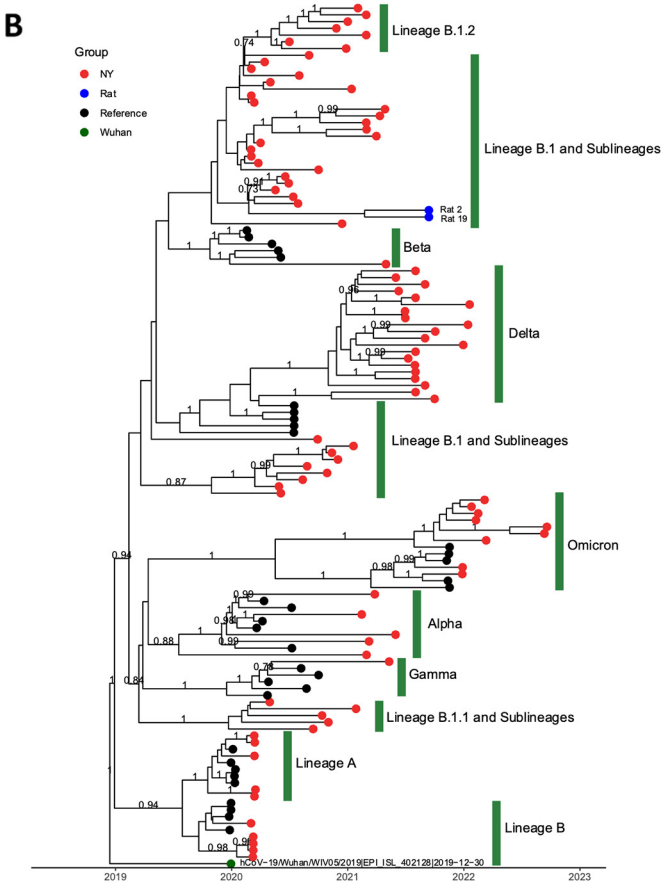

C

	Rat 2	Lineage B	Delta	Omicron	Alpha	Beta	Gamma
Rat 2	--	1	37	38	23	9	16
Lineage B	--	--	36	37	22	8	15
Delta	--	--	--	69	55	43	49
Omicron	--	--	--	--	52	41	45
Alpha	--	--	--	--	--	30	31
Beta	--	--	--	--	--	--	21
Gamma	--	--	--	--	--	--	--

	Rat 19	Lineage B	Delta	Omicron	Alpha	Beta	Gamma
Rat 19	--	2	12	22	14	7	30
Lineage B	--	--	10	20	12	5	28
Delta	--	--	--	28	19	14	37
Omicron	--	--	--	--	25	23	42
Alpha	--	--	--	--	--	17	34
Beta	--	--	--	--	--	--	33
Gamma	--	--	--	--	--	--	--

FIG 1 Genomic sequences of severe acute respiratory syndrome coronavirus 2 (SARS-CoV-2) in wild rats. (A) SARS-CoV-2 genomes found in rats compared with reference wild-type virus and variants of concern. Analyses were performed and visualized using https://clades.nextstrain.org. Reference sequences were downloaded from GISAID. (B) Phylogenetic tree of rat SARS-CoV-2 sequences with reference sequences from wild-type viruses and variants of concern. Branches with a posterior probability of ≥0.7 are labeled. (C) Distance matrices of regions covered by each rat-derived SARS-CoV-2 genome. Lineage B is represented by hCoV-19/Wuhan/IME-WH05/2019|EPI_ISL_529217|2019-12-30, Delta by hCoV-19/USA/NY-Wadsworth-21052117-01/2021|EPI_ISL_2278740|2021-05-01, Omicron by hCoV-19/USA/NY-NYULH1825/2021|EPI_ISL_2427410|2021-05-11, Alpha by hCoV-19/USA/NY-Wadsworth-21070773-01/2021|EPI_ISL_2868594|2021-05-31, and Beta by hCoV-19/USA/NY-PRL-2021_1008_02C08/2021|EPI_ISL_5285364|2021-10-03.

the lungs of all rats infected with any variant at 2 or 4 dpi (Fig. 2F). In line with the viral titers, the rats infected with the Delta variant showed the highest antigen expression in the lungs compared to those infected with other variants (Fig. 2G).

To assess the innate and adaptive immune responses induced by the virus infection in rats, we determined cytokine/chemokine expressions in the lung tissues at 2 and 4 dpi and the antibody titers at 21 dpi. The results showed that all infections induced pro-inflammatory cytokine/chemokine expression (i.e., interferon [IFN]-β, IFN-γ, tumor necrosis factor α, interleukin [IL]-1α, IL-1β, IL-6, CCL-2, IP-10, and IL-10), particularly at 2 dpi (Fig. 3A). The expression of all the cytokines/chemokines induced by the Delta variant was higher than those induced by Alpha and Omicron variants.

Regarding the adaptive immune response, both IgG antibodies and neutralizing

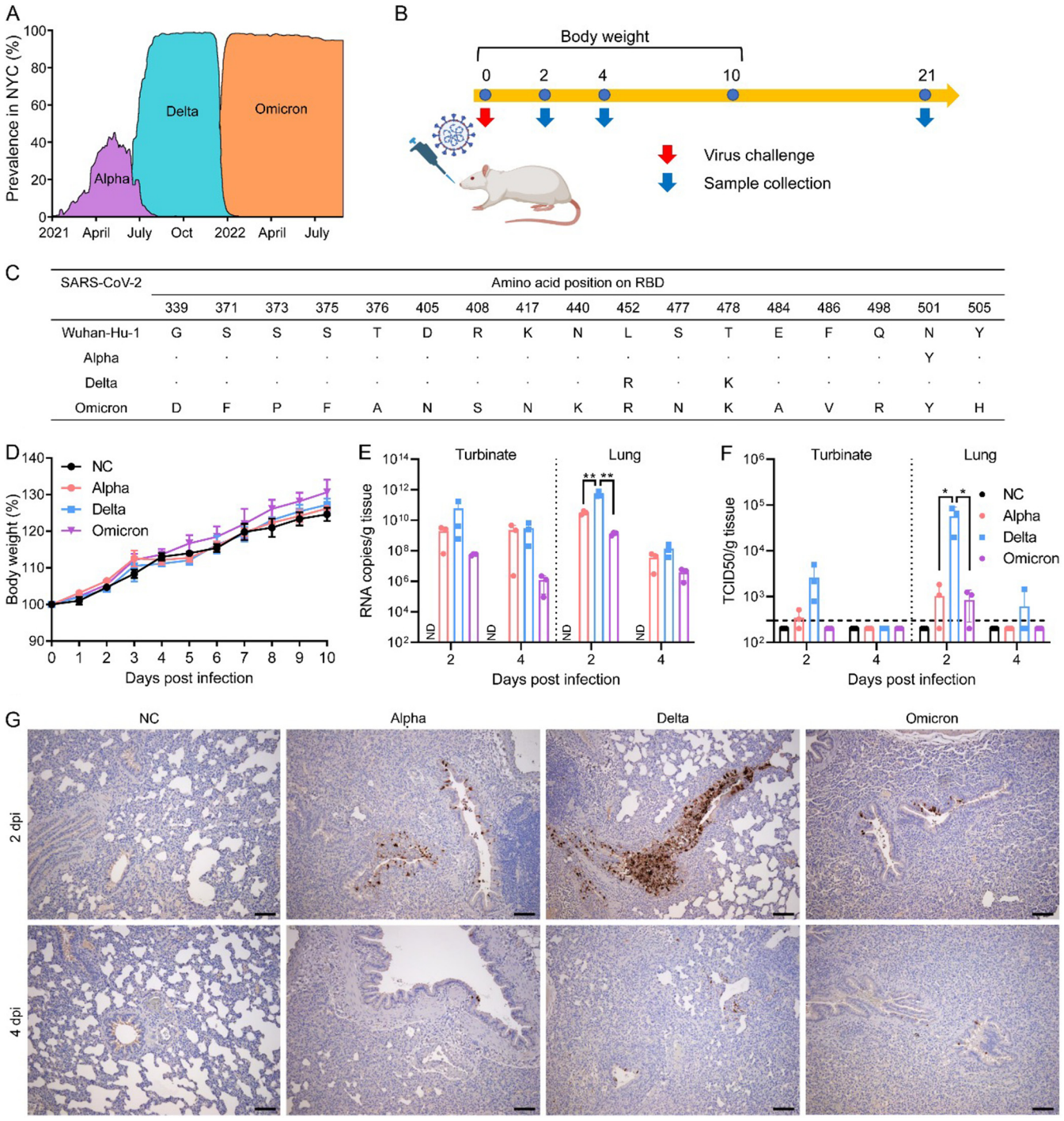

FIG 2 Sprague Dawley (SD) rats are susceptible to infection with Alpha, Delta, and Omicron variants. (A) Prevalence of Alpha, Delta, and Omicron variants in NYC. Figure adapted from https://outbreak.info. (B) Scheme of the virus challenge experiment using 6-week-old SD rats. (C) Amino acid changes of Alpha, Delta, and Omicron variants across the receptor binding domain (RBD) compared to Wuhan-Hu-1 (NCBI access no. MN908947.3). (D) Body weight of rats mock-infected or infected with either Alpha, Delta, or Omicron variant. (E and F) Viral RNA copies (E) and infectious viral titers (F) in the turbinate and lungs from rats infected with either Alpha, Delta, or Omicron variant at 2 or 4 days postinfection (dpi). *, $P < 0.05$; **, $P < 0.01$. (G) Detection of SARS-CoV-2 nucleocapsid protein in bronchial epithelial cells by immunohistochemistry at 2 and 4 dpi. Scale bar = 100 μm.

antibodies were detected for all three variants at 21 dpi; however, IgM antibodies were not detected in any rats regardless of the variant (Fig. 3B and C). There was no significant difference between the Alpha and Delta variants in the IgG antibody titers against Wuhan-Hu-1 spike protein or RBD. However, Delta showed significantly higher anti-RBD IgG titers than Omicron. The homologous neutralizing antibody titers induced by

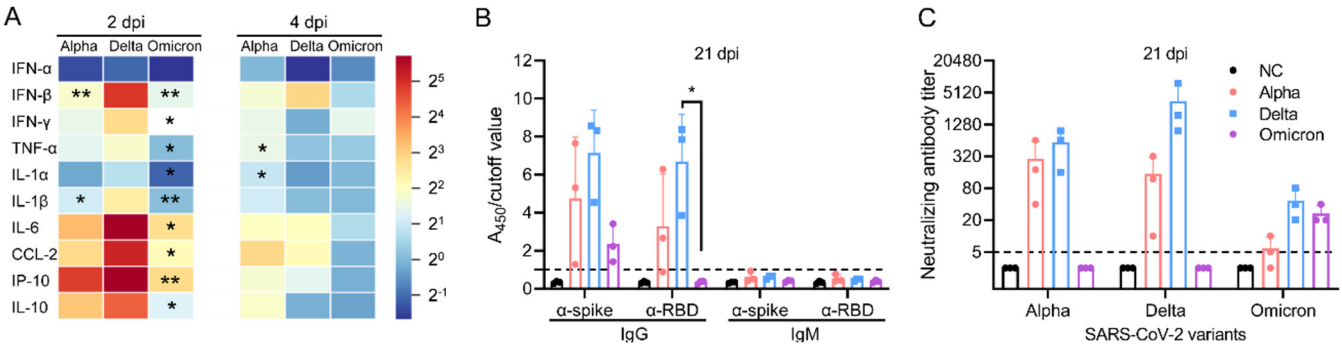

FIG 3 Innate and adapted immune responses induced by SARS-CoV-2 infection in SD rats. (A) Pro-inflammatory cytokine/chemokine expression in lungs from rats infected with either Alpha, Delta, or Omicron variant. Asterisks indicate significant differences between the indicated variant and Delta. *, $P < 0.05$; **, $P < 0.01$. (B) Wuhan-Hu-1 spike protein- or RBD-specific IgG or IgM antibody titers. Absorbance at 450 nm (A_{450})/cutoff was interpreted as negative if ≤1.0 and seropositive if >1.0. The cutoff value was 3-fold of the mean of negative serum samples. (C) Alpha-, Delta-, or Omicron-specific neutralizing antibody titers induced in mock-infected rats or rats infected with either Alpha, Delta, or Omicron variant.

the Delta variant were significantly higher than those induced by Alpha ($P = 0.0441$) or Omicron ($P = 0.0040$). These results indicate that all the three variants can infect SD rats and induce innate and adaptive immune responses, and among these three variants, the Delta variant replicates more efficiently than the Alpha and Omicron variants in rats.

To detect potential host-adapted mutations, we sequenced SARS-CoV-2 in lung tissues from the rats challenged with Alpha, Delta, and Omicron. Our results suggest that there were no adaptive amino acid substitutions along the RBDs across the three testing variants. However, N74K on the spike protein (N-terminal domain) was observed in all animals challenged with Alpha (Table 2). Additional amino acid substitutions in nonstructural protein (NSP)6, NSP13, and the nucleoprotein were observed in some animals challenged by Alpha or Delta. Genomic analyses showed that polymorphisms were observed through these positions in both the challenge strain and the samples collected from rats. Interestingly, most of the samples collected from the rats, particularly at 4 dpi, had identical polymorphism compositions but different polymorphism proportions at these same positions, leading to changes in the consensus sequence and, thus, to the substitutions in the deduced amino acid sequences of the proteins, as shown in Table 2. These results suggest that the majority of those substitutions were derived from purifying selection which occurred after the virus infected the rats. No adaptive mutations were observed in the animals challenged by Omicron.

Structural modeling between RBD of SARS-CoV-2 variants and ACE2 of rat, mouse, and human. To explain the relative replication efficiency of the three SARS-CoV-2 variants in SD rats, we computationally modeled the interactions between rat ACE2 and the RBD of the Alpha, Delta and Omicron variants (Fig. 4) because virus-receptor interaction is often an important determinant of virulence. In our structural models, residue 452 does not directly engage with rat ACE2, but it is surrounded by a large number of nearby residues (Fig. 4C). Therefore, the L452R mutation in the Delta variant could alter the structure conformation of the adjacent β-strand at the ACE2 interface and thus indirectly modulate ACE2 binding affinity (Fig. 4C). Indeed, *in vitro* binding assays indicated that the RBD of the Delta variant, which contains the L452R/T478K double mutation, binds rat ACE2 with a >2-fold stronger affinity than the RBD of Wuhan-Hu-1, the original pandemic virus (15). The enhanced binding of the Delta RBD to rat ACE2 is likely due to L452 alone, because residue 478 is distant from other amino acids, and T478K was found to have no significant effect on binding to mouse ACE2, which is a close homolog of rat ACE2 (16). The Alpha variant also replicates well in rats but is slightly less efficient than Delta. Our structure model shows that the single mutation N501Y in Alpha RBD interacts favorably with H353 on the rat ACE2, with the aromatic side chain of Y501 stacked against the side chain of H453 (Fig. 4D). *In vitro* binding assays confirmed that the Alpha RBD binds rat ACE2 with a >2-fold stronger affinity than RBD of the prototype virus (15), consistent with our structural analysis.

TABLE 2 Deduced amino acid substitutions in SARS-CoV-2 recovered from the lung tissues of rats challenged with SARS-CoV-2 Alpha, Delta, and Omicron variants

	Amino acid residue and allele frequency on viral proteins[b]														
	ORF1a			ORF1b			Spike						Nucleocapsid		
	3718[c]			979[d]			19			74			63		
Variant, strain, and animal ID	Coverage	Amino acid	Percentile	Coverage	Amino acid	Percentile	Coverage	Amino acid	Percentile	Coverage	Amino acid	Percentile	Coverage	Amino acid	Percentile
Alpha															
Challenge strain	4,826	**V**/D/F	99.63/0.17/0.06	2452	**D**/N/Y	98.86/0.90/0.08	7770	**T**/P/A	99.36/0.13/0.12	6507	**N**/K/D	97.88/1.86/0.11	5509	**D**/A/G	99.60/0.13/0.09
SD10 (2 dpi)[a]	3,280	**V**/F/A	99.70/0.09/0.09	2773	**N**/D/S	59.03/40.71/0.11	9363	**T**/X/I	99.21/0.25/0.20	11767	**K**/N/R	72.98/26.64/0.19	19612	**D**/A/G	99.52/0.14/0.12
SD11 (2 dpi)	3,469	**V**/I/A	99.51/0.14/0.12	2759	**N**/D/Y	50.53/48.97/0.14	8601	**T**/X/I	99.16/0.26/0.21	10292	**K**/N/D	68.43/31.29/0.08	18348	**D**/E/G	99.54/0.13/0.10
SD12 (2 dpi)	4,361	**V**/A/G	99.43/0.25/0.11	4070	**D**/N/G	59.21/40.49/0.07	13424	**T**/X/I	99.08/0.27/0.24	16764	**K**/N/D	55.15/44.64/0.05	37262	**D**/A/Y	99.50/0.11/0.09
SD13 (4 dpi)	3,193	**V**/A/G	99.44/0.22/0.13	3380	**N**/D/T	53.05/46.60/0.12	8588	**T**/X/I	99.24/0.34/0.21	11489	**K**/N/E	67.66/31.93/0.13	72592	**D**/G/A	99.33/0.17/0.16
SD14 (4 dpi)	4,248	**V**/A/G	99.36/0.45/0.07	5939	**N**/D/S	66.37/33.34/0.08	8428	**T**/X/I	99.22/0.20/0.15	8715	**K**/N/R	78.03/21.62/0.13	27078	**D**/G/A	99.18/0.24/0.21
SD15 (4 dpi)	4,102	**V**/A/I	99.27/0.37/0.15	4050	**N**/D/G	56.69/42.94/0.10	9807	**T**/X/I	99.14/0.32/0.20	12763	**K**/N/E	71.01/28.64/0.17	49862	**D**/A/I	99.18/0.18/0.17
Delta															
Challenge strain	393	**V**/A/D	52.42/46.82/0.51	3246	**D**/G/N	99.72/0.09/0.09	9420	**R**/T/I	71.20/28.25/0.11	6800	**N**/S/K	99.62/0.18/0.07	5523	**D**/G/A	50.57/49.01/0.13
SD19 (2 dpi)	333	**A**/V/S	54.05/44.74/0.30	3278	**D**/G/Y	99.57/0.18/0.06	7861	**R**/T/X	60.12/39.14/0.23	7870	**N**/D/K	99.49/0.15/0.11	10553	**D**/G/E	59.51/39.96/0.14
SD20 (2 dpi)	441	**A**/V/D	58.96/40.82/0.23	3868	**D**/E/Y	99.61/0.10/0.10	8405	**R**/T/X	67.41/32.02/0.14	7489	**N**/S/I	99.67/0.08/0.07	9115	**D**/G/A	57.03/42.62/0.10
SD21 (2 dpi)	304	**A**/V/D	55.92/43.42/0.66	3168	**D**/G/E	99.56/0.13/0.09	7846	**R**/T/X	68.53/30.92/0.22	6753	**N**/D/S	99.60/0.13/0.10	7656	**D**/G/A	61.01/38.49/0.20
SD22 (4 dpi)	376	**A**/V/G	69.68/30.05/0.27	8071	**D**/G/Y	99.59/0.19/0.10	11981	**T**/R/X	55.88/43.36/0.28	14602	**N**/S/K	99.57/0.14/0.08	34649	**D**/G/A	52.73/46.92/0.15
SD23 (4 dpi)	342	**A**/V/D	66.67/33.04/0.29	6716	**D**/G/N	99.48/0.13/0.10	9494	**T**/R/X	52.34/47.01/0.20	11679	**N**/S/K	99.55/0.15/0.09	28796	**G**/D/A	54.28/45.37/0.09
SD24 (4 dpi)	287	**A**/V/S	71.78/27.53/0.70	7375	**D**/N/Y	99.42/0.27/0.12	9575	**T**/R/X	50.44/48.78/0.29	11203	**N**/S/D	99.37/0.21/0.16	26161	**G**/D/A	50.28/49.30/0.18
Omicron															
Challenge strain	6,233	**V**/D/A	99.61/0.18/0.13	3131	**D**/G/V	99.65/0.16/0.10	6381	**I**/T/V	99.37/0.31/0.14	6896	**N**/T/S	99.65/0.12/0.10	7316	**D**/E/A	99.49/0.18/0.14
SD28 (2 dpi)	9,755	**V**/A/D	99.48/0.24/0.10	10993	**D**/G/Y	99.58/0.14/0.07	7599	**I**/T/V	99.24/0.53/0.08	12231	**N**/S/D	99.70/0.11/0.07	47945	**D**/A/G	99.47/0.12/0.12
SD29 (2 dpi)	6,365	**V**/A/G	99.53/0.16/0.14	6415	**D**/Y/G	99.67/0.12/0.06	5306	I/T/M	99.42/0.41/0.09	7758	**N**/S/K	99.48/0.13/0.12	29364	**D**/A/E	99.44/0.17/0.15
SD30 (2 dpi)	10,010	**V**/D/A	99.66/0.12/0.08	11249	**D**/G/N	99.64/0.12/0.07	7432	**I**/T/M	99.11/0.69/0.09	11270	**N**/S/D	99.59/0.15/0.07	44285	**D**/G/A	99.36/0.16/0.15
SD31 (4 dpi)	5,997	**V**/A/G	99.50/0.35/0.03	7853	**D**/G/N	99.47/0.27/0.10	5190	**I**/T/R	97.86/0.91/0.89	6564	**N**/D/S	99.65/0.12/0.06	31682	**D**/H/I	98.31/0.52/0.39
SD33 (4 dpi)	7,329	**V**/A/G	99.41/0.33/0.10	9266	**D**/G/E	99.57/0.19/0.06	4887	**I**/T/M	98.69/1.06/0.08	8948	**N**/S/D	99.71/0.11/0.04	36052	**D**/G/A	99.32/0.29/0.15

[a]SARS-CoV-2, severe acute respiratory syndrome coronavirus 2; dpi, days postinfection.
[b]Amino acid substitutions compared to the challenge strain are indicated by bold underlined text.
[c]Residue 148 in NSP6, proofreading 3′–5′ exonuclease, N7-methyltransferase.
[d]Residue 56 in NSP13, replication organelle formation.

The Omicron variant has many mutations in its RBD compared to the prototype virus (Fig. 2C). Among these mutations, eight are located near the ACE2 binding interface, including residues 405, 452, 477, 478, 486, 498, 501, and 505. Close inspection of these residues shows favorable interactions by residues R452, N477, R498, Y501, and H505 with the rat ACE compared to their corresponding residues in the prototype strain. Residues D405 and K478 are somewhat spatially distant from the ACE2 interaction sites, while V486 appears to weaken the interaction with rat ACE2 compared to F486 in other SARS-CoV-2 viruses (Fig. 3D).

In conclusion, the spike proteins of the Alpha, Delta and Omicron variants appear to have enhanced binding to the rat ACE2 compared to the prototype virus.

DISCUSSION

Both the serological and molecular data from this study suggest that the rats from NYC were exposed to SARS-CoV-2. Of the tested rats, 16.5% were seropositive, which was higher than the seropositivity rates described in previous reports (11, 12). In addition, 5.1% of these samples were qRT-PCR-positive to SARS-CoV-2, and partial genomes were recovered from all samples which were qRT-PCR-positive for SARS-CoV-2. Genomic analyses suggest that the viruses detected from the collected Norway rats were associated with the B-lineage virus, which was predominant in NYC during the early stages of the pandemic. We speculate that these B-lineage viruses are enzootic in rat populations after being introduced to the NYC rat populations during the early stages of the pandemic, or that rats could have been exposed to the B-lineage viruses present in unknown sources. This is supported by a recent study reporting that the Wuhan-Hu-1-like virus can infect SD rats (17), although an earlier study showed that the prototype Wuhan-Hu-1-like SARS-CoV-2 could not infect SD rats (6). Such a discrepancy may be due to additional mutations in the challenge Wuhan-Hu-1-like strains or genetic variations in the SD rats used in these studies. Thus, further surveillance is needed to understand the virological prevalence in NYC rats, particularly for several emerging variants with high infectivity among rats, including those that circulated in NYC during the past 2 years of the COVID-19 pandemic.

A number of studies have suggested that fragments of SARS-CoV-2 genomes were identified in sewage water systems, and that the prevalence of SARS-CoV-2 in sewage water systems coincides with outbreaks in resident human populations (18). However, no evidence has shown that SARS-CoV-2 viruses in sewage water are infectious (19), suggesting that sewage rats may have been exposed to the virus through airborne transmission, e.g., overlapping living spaces with humans or indirect transmission from unknown fomites, e.g., contaminated human food waste. In a recent study, Zeiss et al. (13) showed that approximately one-quarter of naive rats shed SDAV, another rat respiratory betacoronavirus, following fomite exposure in a controlled laboratory setting. Notably, previously exposed seropositive rats became reinfected with SDAV at similar rates following fomite exposure 114 to 165 days later, indicating that immunity is temporary. In our study, 2 of 4 rats (Rats 2 and 19) were both seropositive and viral RNA-positive, implying that previously exposed seropositive animals may still contract and shed SARS-CoV-2, consistent with prior studies demonstrating breakthrough infections in humans who were previously exposed to SARS-CoV-2 or rats exposed to SDAV (13, 20, 21). Further studies need to evaluate whether rats with prior exposure to SARS-CoV-2 can be reinfected with the same SARS-CoV-2 or a different SARS-CoV-2 variant and whether these breakthrough infections, if present, could facilitate SARS-CoV-2 virus enzoosis in the NYC rat populations.

Although our limited sample size of wild Norway rats revealed detection of only B-lineage viruses, we used animal models to further demonstrate that, in addition to the Alpha and Beta variants which have been previously reported (6–9), Delta and Omicron variants can also cause infections in SD rats. The tested variants also replicated to high levels in both the upper and lower respiratory tracts of rats, although they did not cause any bodyweight loss or other clinical signs. Of the three variants, Delta replicated the most efficiently, while the Omicron variant replicated the least efficiently compared to both Alpha and Delta, although this difference did not reach

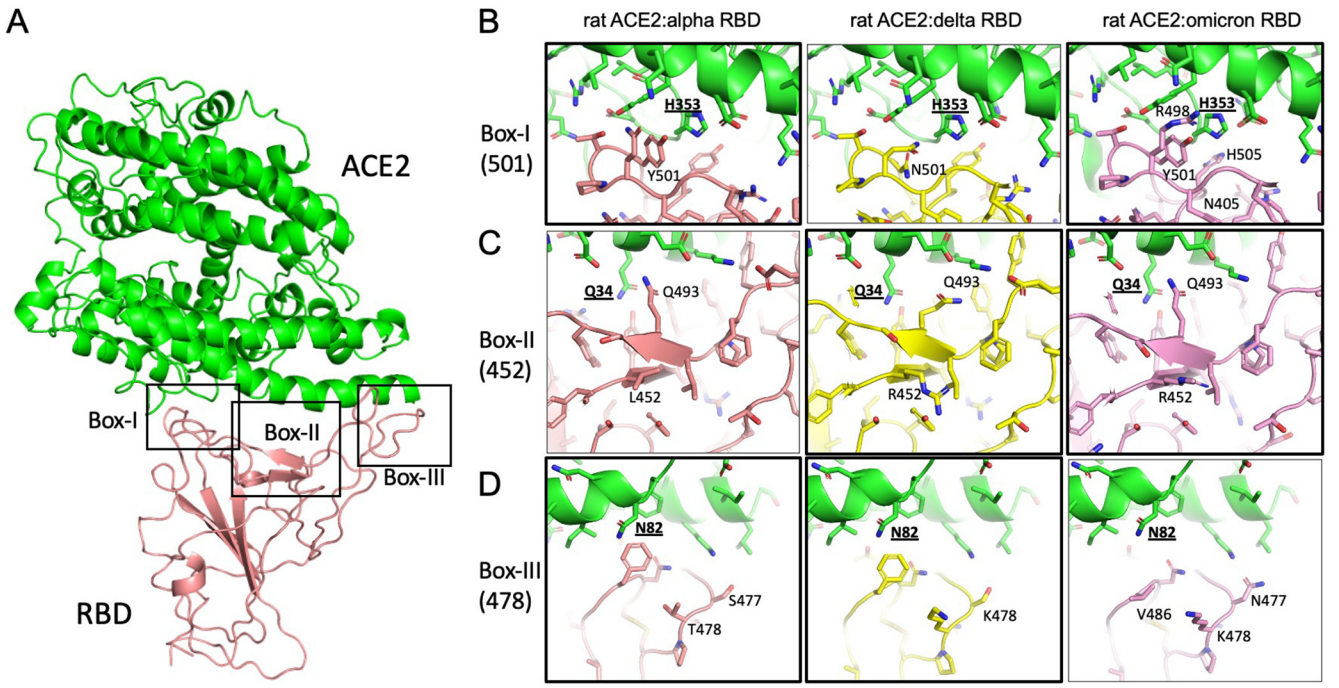

E

ACE2	24	34	82	325	329	353	387
Rat	K	Q	N	P	T	H	K
Mouse	N	Q	S	Q	A	H	R
Human	Q	M	M	Q	E	K	A
	↓	↓	↓			↓	↓
RBD	**477, 478**	**452**	**486**			**501, 498**	**405, 505**

FIG 4 Interactions between the RBD of SARS-CoV-2 variants Alpha, Delta, and Omicron and rat ACE2. (A) Rat ACE2 in complex with RBD. The three major contact sites in box-1, box-2, and box-3 are shown in panels B, C, and D, respectively. Interactions mediated by Alpha, Delta, and Omicron RBDs are compared side-by-side. Black thick outlines highlight favorable interactions. (E) List of ACE2 amino acid variations between rat, mouse, and human at the RBD interface. Many RBD mutations in Alpha, Delta, and Omicron variants are located near host-specfic ACE2 residues, indicated by black arrows.

a statistically significant level between Omicron and Alpha. This finding is consistent with earlier reports that Omicron replicated less efficiently and caused less lung pathology in wild-type or human ACE2 transgenic mice or hamsters compared to other variants (22, 23).

Structural modeling showed that all three variants Alpha, Delta, and Omicron have enhanced binding to SD rat ACE2 compared to the prototype Wuhan-Hu-1-like virus. In light of the biochemical data that Alpha and Delta RBDs bind to rat ACE2 equally well (15), the differences in the replication efficiency that we detected among the three viruses could be due to factors other than receptor binding affinity. It is also interesting to note that many RBD mutations observed in the three variants, such as N501Y in Alpha and L452R/T478K in Delta, interact with ACE2 residues which vary between humans and rats/mice (Fig. 4E). Therefore, rats likely play an important role in the evolution of Alpha, Delta, Omicron variants, which has the potential to result in the emergence of new variants in rats that are naive to the human population and may contain properties harmful to humans. As an example of this occurrence, Zhang et al. (16) proposed that mice could be associated with the emergence of Omicron variants.

In addition to receptor binding, a number of other studies suggested that other structural and nonstructural proteins may play critical roles in viral replication *in vitro* and the host tropism of SARS-CoV-2 viruses. Syed et al. (24) showed that, despite

envelope protein substitutions inhibiting virus assembly, Omicron has an overall higher assembly efficiency than the original SARS-CoV-2, similar to Delta. Bojkova et al. (25, 26) showed that the Omicron variant is less effective in antagonizing the interferon response and has higher sensitivity in interferon treatment than the Delta variant, which may be associated with the substitutions on NSP3, NSP12, NSP13, nucleocapsid, and ORF3 proteins. Interestingly, Omicron did not adapt any observed amino acid substitutions throughout the course of a virus challenge in SD rats, whereas Alpha and Delta did for spike, nucleoprotein, NSP6, and NSP13. The roles of these amino acid substitutions in virus fitness needs to be further studied.

In summary, we found that the rats in the NYC sewage system have been exposed to SARS-CoV-2, and that the Delta and Omicron variants can infect rats in addition to the Alpha and Beta variants. Our findings highlight the potential risk of secondary zoonotic transmission from rats and the need for further monitoring of SARS-CoV-2 in wild rat populations.

MATERIALS AND METHODS

Cells. Vero E6 cells (CRL-1586, American Type Culture Collection [ATCC]) and 293FT/hACE2+TMPRSS (18) were cultured in high glucose Dulbecco's Modified Eagle medium (DMEM, Thermo Fisher Scientific) supplemented with 10% fetal bovine serum (FBS, Thermo Fisher Scientific) at 37°C with 5% CO_2. Rat lung epithelial cells L2 (CCL-149, ATCC) were cultured in F-12K Medium (ATCC) supplemented with 10% FBS at 37°C with 5% CO_2. Rat primary tracheal epithelial cells (Cell Biologics) were grown on culture flasks or plates pre-coated with gelatin-based coating solution (Cell Biologics) in Complete Epithelial Cell Medium (Cell Biologics) at 37°C with 5% CO_2.

Viruses. The SARS-CoV-2/USA/CA_CDC_5574/2020 (Alpha, B.1.1.7, NR-54011, BEI Resources), and SARS-CoV-2/human/USA/MD-HP05285/2021 (Delta, B.1.617.2, NR-55671, BEI Resources) were propagated in Vero E6 cells. The SARS-CoV-2/USA/MO-CV40709/2022 (Omicron, BA.5.5, GISAID accession no. EPI_ISL_15823386) was recovered from human nasopharyngeal swab and propagated on Vero E6 cells.

Virus challenge in rats. Sprague Dawley rats are an outbred strain of albino laboratory rats belonging to *Rattus norvegicus*, the same species as Norway rats. SD rats have been widely used for studying coronaviruses in rat populations and share identical ACE2 receptors to Norway rats. Thus, SD rats were used as the animal model. Six-week-old female specific-pathogen-free SD rats were purchased from Charles River Laboratories and were each separately housed in individually ventilated cages (GR900 for rats, Green Line, Techniplast) in the animal biosafety level 3 (ABSL-3) laboratory at the University of Missouri-Columbia. SD rats were anesthetized with isoflurane, followed by intranasal inoculation via both nostrils (half-volume each) with 2×10^4 PFU/rat of SARS-CoV-2 diluted in 50 μL phosphate-buffered saline (PBS). Clinical evaluation was performed daily, and body weight was determined daily through 10 dpi. At 2, 4, and 21 dpi, animals were euthanized for blood and tissue collection for seroconversion evaluation, viral load titration, and histology staining. Blood drawn from rats by cardiac puncture with 5-mL syringes and 23-G needles was collected into 2-mL microcentrifuge tubes (USA Scientific). The rat sera were obtained by placing the blood at room temperature for 3 h to clot, followed by centrifugation at 5,000 $\times$ *g* for 10 min at 4°C.

Wild rat capture and sample collection. In the fall of 2021, APHIS Wildlife Services conducted sampling of Norway rats (*Rattus norvegicus*) in New York City to look for evidence of SARS-CoV-2 infection. In locations surrounding wastewater systems, two trapping efforts during September and November were conducted with permission from the NYC Department of Parks and Recreation. Each effort consisted of 3 days of pre-baiting followed by four nights of trapping. Most animals were captured in city parks within the borough of Brooklyn, although some were captured near buildings outside park boundaries. Once the animals were euthanized, biologists collected and processed fresh blood samples. Over the course of eight trapping nights, 79 rats were trapped and sampled. Serum samples along with the carcasses were shipped to the Wildlife Services National Wildlife Disease Program in Fort Collins, Colorado, where tissues were extracted and sent to the University of Missouri for additional testing.

Homogenization of animal issues. Animal tissues were homogenized in maintenance medium for 1 min at 6,000 rpm using a homogenizer (Bertin, Precellys). The maintenance medium was made with high-glucose DMEM (Thermo Fisher Scientific), 7.5% bovine serum albumin (BSA, final concentration of 0.3%, Sigma-Aldrich) and penicillin/streptomycin (final concentration of 1%, Thermo Fisher Scientific). Following homogenization, the debris were pelleted by centrifugation for 10 min at 12,000 $\times$ *g*. The supernatants were collected for viral titration, virus isolation, and/or viral RNA extraction.

Infectious viral titration by $TCID_{50}$. The infectious virus titers were determined by $TCID_{50}$ with Vero E6 cells. In brief, the samples were half-log serially diluted on 96-well plates with maintenance medium, and 4 replicates of each sample were performed. Next, 3×10^4 Vero E6 cells were added to each well. Following a 2-day incubation at 37°C with 5% CO_2, the culture medium in each well was discarded and the cells were treated with 4% paraformaldehyde solution (Santa Cruz Biotechnology, Inc.) to fix the cells and inactivate the virus. The cells were then treated by 0.1% TritonX-100 (Sigma-Aldrich) and strained with monoclonal rabbit antibody against SARS-CoV-2 nucleocapsid (Sino Biological). This was subsequently detected by the addition of horseradish peroxidase (HRP)-conjugated goat anti-rabbit IgG (Thermo Fisher Scientific) and TMB-ELISA substrate (Thermo Fisher Scientific). Optical density at 450 nm (OD_{450}) was measured by Cytation 5 (Bio-Tek). The well was determined as positive if its OD_{450} was

higher than the cutoff value (mean OD_{450} of cell control wells multiplied by 2). The 50% tissue culture infective dose ($TCID_{50}$) was calculated using the Reed and Muench method.

Viral RNA detection. RNA was extracted from the tissue homogenates using a GeneJet viral DNA/RNA purification kit (Thermo Fisher Scientific) or a MagMax Pathogen RNA/DNA kit (Thermo Fisher Scientific). The viral RNA was detected and quantified by qRT-PCR using a SARS-CoV-2 diagnostic panel consisting of N1 (forward primer sequence, 5′-GAC CCC AAA ATC AGC GAA AT-3′; reverse primer sequence, 5′-TCT GGT TAC TGC CAG TTG AAT CTG-3′; probe sequence, 5′-ACC CCG CAT TAC GTT TGG TGG ACC-3′) and/or N2 primer/probe mix (forward primer sequence, 5′-TTACAAACATTGGCCGCAAA-3′; reverse primer sequence, 5′-GCGCGACATTCCGAAGAA-3′; probe sequence, 5′-ACAATTTGCCCCCAG CGCTTCAG-3′) (27). The qRT-PCR was performed using TaqMan Fast Virus 1-Step Master Mix according to the manufacturer's protocol (Thermo Fisher Scientific). Fluorescent signals were acquired using a QuantStudio 6 real-time PCR system (Thermo Fisher Scientific). Viral load was calculated based on the standard curve established by serial dilution of a 2019-CoV N positive-control plasmid (IDT).

Measurement of cytokine/chemokine expression. Total RNA was extracted from rat tissues by using a combination method which utilizes TRIzol (Thermo Fisher Scientific) and an RNeasy Minikit (Qiagen) (28). The genomic DNA was removed by on-column DNase I (Qiagen) treatment during the RNA extraction. The RNA was then reverse-transcribed into cDNA with SuperScript III Reverse Transcriptase with random hexamer primers (Thermo Fisher Scientific). The cDNA was used in real-time PCR with PowerUp SYBR Green Master Mix (Thermo Fisher Scientific) for specific targets (Table S3). The expression of housekeeping gene GAPDH was used to normalize the amount of RNA isolated from tissues. The threshold cycle ($2^{-\Delta\Delta CT}$) method was used to compare the differential gene expressions between testing samples. The mean fold change ($2^{-\Delta\Delta CT}$) values of triplicates and standard deviation are shown.

Genome sequencing of SARS-CoV-2 viruses. SARS-CoV-2 whole-genome sequencing was performed using a QIAseq DIRECT SARS-CoV-2 kit (Qiagen). The quality of paired-end reads obtained from MiSeq sequencing was analyzed using Qiagen CLC Genomics Workbench 22.0.1 and the Identify ARTIC V3 SARS-CoV-2 Low Frequency and Shared Variants (Illumina) workflow was used for genetic variant analyses. Nucleotide sequences were aligned using MAFFT v7.471, and the mutations were analyzed using Nextclade (https://clades.nextstrain.org). SARS-CoV-2 sequences were recovered directly from the supernatants of the homogenized tissues.

Pan-viral genomic sequencing. To identify any coronaviruses and other types of pathogens present in the rat samples we collected from NYC, pan-viral target hybridization enrichment sequencing was performed using RNA Prep with an Enrichment (L) Tagmentation kit (Illumina) and the Comprehensive Viral Research Panel according to the manufacturer's manual (Twist Biosciences). The Twist Comprehensive Viral Research Panel from Twist Biosciences has >1 million unique probes targeting 3,153 viral genomes (15,488 different strains), including those reported in the virus family *Coronaviridae*.

Phylogenetic analyses and molecular characterization. Time-scaled phylogenetic trees were generated using the two rat samples containing >10% coverage (Rats 2 and 19), five reference sequences for each variant of concern (Alpha, Beta, Delta, Gamma, and Omicron), five reference sequences for lineage A and lineage B viruses, and three randomly selected NYC sequences from each month. Phylogenetic analyses were performed using BEAST v2.7.0 with the Hasegawa, Kishino, and Yano (HKY) + Γ_4 substitution model, an exponential coalescent growth prior, and a strict molecular clock. Independent runs were performed with chain lengths of 10,000,000 steps and sampled every 5,000 steps per run with a 10% burn-in. The resulting trees were summarized with TreeAnnotator and visualized using FigTree. A posterior probabilities cutoff of 0.70 was used to assess tree topology.

Virus isolation. Virus isolation was attempted in Vero E6 cells, 293FT/hACE2 + TMPRSS, L2, or rat primary tracheal epithelial cells. Here, 200 μL of supernatant from homogenized tissues was mixed with an equal volume of cell culture medium and then inoculated onto pre-seeded cells in 6-well plates. After 1 h of adsorption, the inoculum was removed, and the cells were washed with PBS and covered with fresh cell culture medium. The cells were monitored daily for cytopathogenic effects (CPE) and the supernatants were harvested at 3 to 5 dpi. The supernatants were inoculated onto fresh cells for a maximum of 3 times until CPE were observed. The supernatants from the last inoculation were subjected to viral RNA extraction and SARS-CoV-2 specific real-time RT-PCR using SARS-CoV-2 diagnostic panels.

ELISA. Anti-SARS-CoV-2 spike and anti-SARS-CoV-2 receptor binding domain IgG or IgM antibodies were determined using stabilized spike protein (NR-53524, BEI Resources) or RBD (NR-53366, BEI resources) of SARS-CoV-2, respectively. The proteins were coated on 96-well ELISA plates (Nunc-Immuno, Thermo Fisher Scientific) at a concentration of 1 μg/mL in PBS. The plates were then blocked with 100 μL of 1% BSA (Research Products International) buffered in PBS containing 0.1% Tween 20 (PBST) and incubated at room temperature for 1 h. Next, 1:100 diluted rat serum samples were added to the plates for 1 h of incubation at 37°C. After extensive washing with PBST, HRP-conjugated goat anti-rat IgG (1:8,000) or anti-rat IgM (1:8,000, Thermo Fisher Scientific) was added for 1 h at 37°C. Following five washes with PBST, 100 μL of TMB-ELISA substrate (1-Step; Thermo Fisher Scientific) was added to each well. After a 15-min incubation, the reaction was stopped by adding 100 μL of 1 M H_2SO_4 solution and the OD_{450} was read using a Cytation 5 Cell Imaging Multimode Reader (Bio-Tek Instruments). The cutoff value was determined based on a signal-to-noise ratio of 3, which is reflected by the mean background reactivity of all serum samples from naive SD rats multiplied by 3. The pooled sera collected from two ferrets infected with ancestral SARS-CoV-2 virus at 4 weeks postinfection served as a positive control.

Microneutralization assay. The serum samples were heat-inactivated at 56°C for 1 h and then 2-fold serially diluted with a starting dilution of 1:5. The serum dilutions were mixed with equal volumes of 100

$TCID_{50}$ SARS-CoV-2 viruses in a 96-well plate, followed by 1 h of incubation at 37°C. Next, 3.5×10^4 Vero E6 cells were added to each well with the serum-virus mixture. The plates were incubated for 2 days at 37°C in 5% CO_2, and the cells were then fixed in 10% paraformaldehyde, penetrated by 0.1% TritonX-100, and strained with monoclonal rabbit antibody against SARS-CoV-2 nucleocapsid (Sino Biological). This was subsequently detected by the addition of HRP-conjugated goat anti-rabbit IgG and TMB-ELISA substrate (Thermo Fisher Scientific). The OD_{450} was measured using a Cytation 5 (Bio-Tek). The serum neutralizing titer is the reciprocal of the highest dilution resulting in an infection reduction of >50%.

Structure modeling. The tertiary structure of the rat ACE2 (NP_001012006.1) was predicted by Alphafold2 using the Google colab server (https://colab.research.google.com/) (29). The RBD structures of Alpha (SARS-CoV-2/USA/CA_CDC_5574/2020, B.1.1.7), Delta (SARS-CoV-2/human/USA/MD-HP05285/2021, B.1.617.2), and Omicron (SARS-CoV-2/USA/MO-CV40709/2022, BA.5.5) were taken from the PDB IDs 7FBK, 7URQ, and 7XWA, respectively. To model the rat ACE2:RBD complex structure, a rat ACE2 structural model and the structure of each of the three RDB domains were superposed onto their respective homologs in PDB ID 7XO9, the SARS-CoV-2 Omicron BA.2 variant RBD complexed with human ACE2 (30) using PyMOL (PyMOL Molecular Graphics System v2.0, Schrödinger, LLC). The resulting complex structures were subjected to energy minimization using Phenix (31). Structure figures were prepared using PyMOL.

Statistical analysis. Statistical significance was tested using a one-way analysis of variance (ANOVA) with Tukey's multiple comparisons by GraphPad Prism v9.1.0.

Ethics statement. Rats were captured in Brooklyn under a wildlife damage management agreement between USDA/APHIS Wildlife Services and the New York City Department of Parks and Recreation. The animal experiments were performed under protocol no. 38742 approved by the Care and Use of Laboratory Animals of the University of Missouri per the USDA Animal Welfare Regulations. All experiments involving live viruses were performed in an approved biosafety level 3 (BSL-3) or ABSL-3 facility at the Laboratory of Infectious Diseases, University of Missouri-Columbia, under protocol no. 20-14, in compliance with the Institutional Biosafety Committee of the University of Missouri-Columbia.

Data availability. We have submitted the following raw and assembled genomic data collected from this study to GenBank under the BioProject accession no. PRJNA924317: (i) data derived from the lung tissues of Rats 2, 19, 43, and 46 by Illumina (Table S1), (ii) data derived from the lung tissues of Rats 2, 19, 30, 38, and 43 (Table S2), and (iii) data derived from the viruses used to infect animals and the lung tissues from experimental animals (Table 2).

All publicly available sequences and associated metadata used in the data set used in our study are published in GISAID's EpiCoV database. To view the contributors of each individual sequence with details such as accession number, virus name, collection date, originating lab and submitting lab, and the list of authors, please visit the doi listed with each data set. GISAID identifier EPI_SET_221019xq (https://epicov.org/epi3/epi_set/221019xq?main=true) is composed of 49 individual genome sequences. The collection dates range from 24 December 2019 to 17 November 2021; data were collected in 11 countries and territories.

SUPPLEMENTAL MATERIAL

Supplemental material is available online only.

TABLE S1, DOCX file, 0.02 MB.

TABLE S2, DOCX file, 0.02 MB.

TABLE S3, DOCX file, 0.02 MB.

ACKNOWLEDGMENTS

This study was supported by USDA American Rescue Plan funding and the National Institute of Allergy and Infectious Diseases of the National Institutes of Health under award no. F30AI172230. We thank George Sarafianos, Rebecca Patterson, and Haley Hudson for their assistance in this study. We thank Marc Johnson for suggesting the wastewater systems targeted in this study and Mark Jacking, John Pistone, Raven Shuman, Deana Brabant Oatman, Maxwell Tanner, Jack Ramirez, Allen Gosser, Bobby Corrigan, Tim Linder, and Tom Gidlewski for wild rat capture, sample collection, and necropsy/tissue processing. We also thank Samantha Gerb, Sarah Schlink, Charles Moley, and Shakera Fudge for their technical support with the animal experiments.

The findings and conclusions in this publication are those of the author(s) and should not be construed to represent any official USDA, National Institutes of Health, or U.S. Government determination or policy.

X.-F.W., J.L., D.K., and T.D. conceived the experiments. X.-F.W., J.L., D.K., T.D., and Y.W. designed the experiments. J.L., D.K., and T.D. contributed to the wild rat capture. Y.W., T.L., J.T., and M.G. performed the experiments. S.C. and C.Z. provided study materials. Y.W., C.T., J.T., T.L., and J.H. analyzed the data. Y.W. and X.-F.W. prepared the original draft. All authors contributed substantially to the revision of this paper.

The authors declare that they have no competing interests.

REFERENCES

1. Johns Hopkins University of Medicine. 2022. Coronavirus resource center. Available from https://coronavirus.jhu.edu/data. Accessed 10 October 2022. Johns Hopkins University, Baltimore, MD.
2. Cui S, Liu Y, Zhao J, Peng X, Lu G, Shi W, Pan Y, Zhang D, Yang P, Wang Q. 2022. An updated review on SARS-CoV-2 infection in animals. Viruses 14:1527. https://doi.org/10.3390/v14071527.
3. Chandler JC, Bevins SN, Ellis JW, Linder TJ, Tell RM, Jenkins-Moore M, Root JJ, Lenoch JB, Robbe-Austerman S, DeLiberto TJ, Gidlewski T, Kim TM, Shriner SA. 2021. SARS-CoV-2 exposure in wild white-tailed deer (*Odocoileus virginianus*). Proc Natl Acad Sci U S A 118:e2114828118. https://doi.org/10.1073/pnas.2114828118.
4. Hale VL, Dennis PM, McBride DS, Nolting JM, Madden C, Huey D, Ehrlich M, Grieser J, Winston J, Lombardi D, Gibson S, Saif L, Killian ML, Lantz K, Tell RM, Torchetti M, Robbe-Austerman S, Nelson MI, Faith SA, Bowman AS. 2022. SARS-CoV-2 infection in free-ranging white-tailed deer. Nature 602:481–486. https://doi.org/10.1038/s41586-021-04353-x.
5. Hammer AS, Quaade ML, Rasmussen TB, Fonager J, Rasmussen M, Mundbjerg K, Lohse L, Strandbygaard B, Jorgensen CS, Alfaro-Nunez A, Rosenstierne MW, Boklund A, Halasa T, Fomsgaard A, Belsham GJ, Botner A. 2021. SARS-CoV-2 transmission between mink (*Neovison vison*) and humans, Denmark. Emerg Infect Dis 27:547–551. https://doi.org/10.3201/eid2702.203794.
6. Shuai H, Chan JF, Yuen TT, Yoon C, Hu JC, Wen L, Hu B, Yang D, Wang Y, Hou Y, Huang X, Chai Y, Chan CC, Poon VK, Lu L, Zhang RQ, Chan WM, Ip JD, Chu AW, Hu YF, Cai JP, Chan KH, Zhou J, Sridhar S, Zhang BZ, Yuan S, Zhang AJ, Huang JD, To KK, Yuen KY, Chu H. 2021. Emerging SARS-CoV-2 variants expand species tropism to murines. EBioMedicine 73:103643. https://doi.org/10.1016/j.ebiom.2021.103643.
7. Pan T, Chen R, He X, Yuan Y, Deng X, Li R, Yan H, Yan S, Liu J, Zhang Y, Zhang X, Yu F, Zhou M, Ke C, Ma X, Zhang H. 2021. Infection of wild-type mice by SARS-CoV-2 B.1.351 variant indicates a possible novel cross-species transmission route. Signal Transduct Target Ther 6:420. https://doi.org/10.1038/s41392-021-00848-1.
8. Zhang C, Cui H, Li E, Guo Z, Wang T, Yan F, Liu L, Li Y, Chen D, Meng K, Li N, Qin C, Liu J, Gao Y, Zhang C. 2022. The SARS-CoV-2 B.1.351 Variant Can Transmit in Rats But Not in Mice. Front Immunol 13:869809. https://doi.org/10.3389/fimmu.2022.869809.
9. Montagutelli X, Prot M, Levillayer L, Salazar EB, Jouvion G, Conquet L, Beretta M, Donati F, Albert M, Gambaro FJB. 2021. Variants with the N501Y mutation extend SARS-CoV-2 host range to mice, with contact transmission. bioRxiv. https://doi.org/10.1101/2021.03.18.436013.
10. Bosco-Lauth AM, Root JJ, Porter SM, Walker AE, Guilbert L, Hawvermale D, Pepper A, Maison RM, Hartwig AE, Gordy P, Bielefeldt-Ohmann H, Bowen RA. 2021. Peridomestic mammal susceptibility to severe acute respiratory syndrome coronavirus 2 infection. Emerg Infect Dis 27:2073–2080. https://doi.org/10.3201/eid2708.210180.
11. Miot EF, Worthington BM, Ng KH, de Lataillade LG, Pierce MP, Liao Y, Ko R, Shum MH, Cheung WY, Holmes EC, Leung KS, Zhu H, Poon LL, Peiris MJ, Guan Y, Leung GM, Wu JT, Lam TT. 2022. Surveillance of rodent pests for SARS-CoV-2 and other coronaviruses, Hong Kong. Emerg Infect Dis 28:467–470. https://doi.org/10.3201/eid2802.211586.
12. Colombo VC, Sluydts V, Marien J, Vanden Broecke B, Van Houtte N, Leirs W, Jacobs L, Iserbyt A, Hubert M, Heyndrickx L, Goris H, Delputte P, De Roeck N, Elst J, Arien KK, Leirs H, Gryseels S. 2022. SARS-CoV-2 surveillance in Norway rats (*Rattus norvegicus*) from Antwerp sewer system, Belgium. Transbound Emerg Dis 69:3016–3021. https://doi.org/10.1111/tbed.14219.
13. Zeiss CJ, Asher JL, Vander Wyk B, Allore HG, Compton SR. 2021. Modeling SARS-CoV-2 propagation using rat coronavirus-associated shedding and transmission. PLoS One 16:e0260038. https://doi.org/10.1371/journal.pone.0260038.
14. Compton SR, Smith AL, Gaertner DJ. 1999. Comparison of the pathogenicity in rats of rat coronaviruses of different neutralization groups. Lab Anim Sci 49:514–518.
15. Yao W, Ma D, Wang H, Tang X, Du C, Pan H, Li C, Lin H, Farzan M, Zhao J, Li Y, Zhong G. 2021. Effect of SARS-CoV-2 spike mutations on animal ACE2 usage and in vitro neutralization sensitivity. bioRxiv. https://doi.org/10.1101/2021.01.27.428353.
16. Zhang W, Shi K, Geng Q, Ye G, Aihara H, Li F. 2022. Structural basis for mouse receptor recognition by SARS-CoV-2 omicron variant. Proc Natl Acad Sci U S A 119:e2206509119. https://doi.org/10.1073/pnas.2206509119.
17. Yu D, Long Y, Xu L, Han JB, Xi J, Xu J, Yang LX, Feng XL, Zou QC, Qu W, Lin J, Li MH, Yao YG. 2022. Infectivity of SARS-CoV-2 and protection against reinfection in rats. Zool Res 43:945–948. https://doi.org/10.24272/j.issn.2095-8137.2022.339.
18. Smyth DS, Trujillo M, Gregory DA, Cheung K, Gao A, Graham M, Guan Y, Guldenpfennig C, Hoxie I, Kannoly S, Kubota N, Lyddon TD, Markman M, Rushford C, San KM, Sompanya G, Spagnolo F, Suarez R, Teixeiro E, Daniels M, Johnson MC, Dennehy JJ. 2022. Tracking cryptic SARS-CoV-2 lineages detected in NYC wastewater. Nat Commun 13:635. https://doi.org/10.1038/s41467-022-28246-3.
19. Robinson CA, Hsieh HY, Hsu SY, Wang Y, Salcedo BT, Belenchia A, Klutts J, Zemmer S, Reynolds M, Semkiw E, Foley T, Wan X, Wieberg CG, Wenzel J, Lin CH, Johnson MC. 2022. Defining biological and biophysical properties of SARS-CoV-2 genetic material in wastewater. Sci Total Environ 807:150786. https://doi.org/10.1016/j.scitotenv.2021.150786.
20. Kellam P, Barclay W. 2020. The dynamics of humoral immune responses following SARS-CoV-2 infection and the potential for reinfection. J Gen Virol 101:791–797. https://doi.org/10.1099/jgv.0.001439.
21. Tang CY, Wang Y, McElroy JA, Li T, Hammer R, Ritter D, Lidl GM, Webby R, Hang J, Wan XF. 2021. Reinfection with two genetically distinct SARS-CoV-2 viruses within 19 days. J Med Virol 93:5700–5703. https://doi.org/10.1002/jmv.27154.
22. Halfmann PJ, Iida S, Iwatsuki-Horimoto K, Maemura T, Kiso M, Scheaffer SM, Darling TL, Joshi A, Loeber S, Singh G, Foster SL, Ying B, Case JB, Chong Z, Whitener B, Moliva J, Floyd K, Ujie M, Nakajima N, Ito M, Wright R, Uraki R, Warang P, Gagne M, Li R, Sakai-Tagawa Y, Liu Y, Larson D, Osorio JE, Hernandez-Ortiz JP, Henry AR, Ciuoderis K, Florek KR, Patel M, Odle A, Wong LR, Bateman AC, Wang Z, Edara VV, Chong Z, Franks J, Jeevan T, Fabrizio T, DeBeauchamp J, Kercher L, Seiler P, Gonzalez-Reiche AS, Sordillo EM, Chang LA, van Bakel H, Consortium Mount Sinai Pathogen Surveillance (PSP) study group, et al. 2022. SARS-CoV-2 Omicron virus causes attenuated disease in mice and hamsters. Nature 603:687–692. https://doi.org/10.1038/s41586-022-04441-6.
23. Yuan S, Ye Z-W, Liang R, Tang K, Zhang AJ, Lu G, Ong CP, Man Poon VK, Chan CC-S, Mok BW-Y, Qin Z, Xie Y, Chu AW-H, Chan W-M, Ip JD, Sun H, Tsang JO-L, Yuen TT-T, Chik KK-H, Chan CC-Y, Cai J-P, Luo C, Lu L, Yip CC-Y, Chu H, To KK-W, Chen H, Jin D-Y, Yuen K-Y, Chan JF-W. 2022. Pathogenicity, transmissibility, and fitness of SARS-CoV-2 Omicron in Syrian hamsters. Science 377:428–433. https://doi.org/10.1126/science.abn8939.
24. Syed AM, Ciling A, Taha TY, Chen IP, Khalid MM, Sreekumar B, Chen PY, Kumar GR, Suryawanshi R, Silva I, Milbes B, Kojima N, Hess V, Shacreaw M, Lopez L, Brobeck M, Turner F, Spraggon L, Tabata T, Ott M, Doudna JA. 2022. Omicron mutations enhance infectivity and reduce antibody neutralization of SARS-CoV-2 virus-like particles. Proc Natl Acad Sci U S A 119:e2200592119. https://doi.org/10.1073/pnas.2200592119.
25. Bojkova D, Widera M, Ciesek S, Wass MN, Michaelis M, Cinatl J, Jr. 2022. Reduced interferon antagonism but similar drug sensitivity in Omicron variant compared to Delta variant of SARS-CoV-2 isolates. Cell Res 32:319–321. https://doi.org/10.1038/s41422-022-00619-9.
26. Bojkova D, Rothenburger T, Ciesek S, Wass MN, Michaelis M, Cinatl J, Jr. 2022. SARS-CoV-2 Omicron variant virus isolates are highly sensitive to interferon treatment. Cell Discov 8:42. https://doi.org/10.1038/s41421-022-00408-z.
27. CDC. 2021. CDC 2019-Novel Coronavirus (2019-nCoV) real-time RT-PCR diagnostic panel. Available from https://www.fda.gov/media/134922/download. Accessed 1 Oct 2021. CDC, Atlanta, GA.
28. Untergasser A. 2008. RNAprep: Trizol combined with columns. Available from http://www.molbi.de/protocols/rna_prep_comb_trizol_v1_0.htm. Accessed 13 April 2021.
29. Mirdita M, Schutze K, Moriwaki Y, Heo L, Ovchinnikov S, Steinegger M. 2022. ColabFold: making protein folding accessible to all. Nat Methods 19:679–682. https://doi.org/10.1038/s41592-022-01488-1.
30. Xu Y, Wu C, Cao X, Gu C, Liu H, Jiang M, Wang X, Yuan Q, Wu K, Liu J, Wang D, He X, Wang X, Deng SJ, Xu HE, Yin W. 2022. Structural and biochemical mechanism for increased infectivity and immune evasion of Omicron BA.2 variant compared to BA.1 and their possible mouse origins. Cell Res 32:609–620. https://doi.org/10.1038/s41422-022-00672-4.
31. Liebschner D, Afonine PV, Baker ML, Bunkoczi G, Chen VB, Croll TI, Hintze B, Hung LW, Jain S, McCoy AJ, Moriarty NW, Oeffner RD, Poon BK, Prisant MG, Read RJ, Richardson JS, Richardson DC, Sammito MD, Sobolev OV, Stockwell DH, Terwilliger TC, Urzhumtsev AG, Videau LL, Williams CJ, Adams PD. 2019. Macromolecular structure determination using X-rays, neutrons and electrons: recent developments in Phenix. Acta Crystallogr D Struct Biol 75:861–877. https://doi.org/10.1107/S2059798319011471.